Proposal of Electrically Reversal Magnetic Pole Type Variable Magnetic Flux PM Motor

Masahiro Aoyama, and Kazukiyo Nakajima
SUZUKI Motor Corporation
300 Takatsuka-cho, Minami-ku, Hamamatsu,
Shizuoka 432-8611, Japan
aoyamam@hhq.suzuki.co.jp
nakajimak@hhq.suzuki.co.jp

Toshihiko Noguchi
Shizuoka University
3-5-1 Johoku, Naka-ku, Hamamatsu,
Shizuoka 432-8561, Japan
noguchi.toshihiko@shizuoka.ac.jp

***Abstract*—This paper describes a variable magnetic flux PM motor in which space harmonic power is utilized for the magnetic flux weakening, automatically. The stator has a toroidally-concentrated winding structure, and the torque generation surfaces are composed of three air-gaps which are single radial-gap and double axial-gaps. The radial-gap rotor is a consist-magnetized PM rotor and the axial-gap rotors are self-excited wound-field rotor. The axial-gap rotor can retrieve a space harmonic power, which is inevitably generated by a concentrated winding structure, for magnetomotive force. A mechanical design of the prototype is revealed, and the operation principle of the automated-magnetic flux weakening is clarified through the FE-analysis. In addition, actual prototype machine is introduced. Consequently, the effect of automated-armature line voltage decrease is investigated with respect to rotation speed increase.**

Keywords—variable magnetic flux; toroidal winding; reversal magnetic pole; multi-gap; self-excited wound field; concentrated winding.

I. INTRODUCTION

A sustainable transportation system can be achieved through the development of higher-efficiency vehicles with significantly lower fuel consumption [1]. Recently, the new standards are achievable with electrified powertrains utilizing electric motors. Electric motors have much higher efficiencies than an ICEs and, thus, require less energy. Interior Permanent Magnet Synchronous Machines (IPMSM) are employed in the most of the currently available hybrid and electric vehicles on the market. Generally, permanent magnet (PM) machines can generate high torque density with the use of high-energy and high-coercivity, competing well against other motor technologies, i.e., an induction machine, a switched reluctance machine. Thus, the greater magnetic flux density and the lower current required to generate a given torque. However, a consequence of increasing flux density of such machines have a higher back EMF constant, which is a linear product of the flux density and the rotation speed.

To solve the drawback of that problem, variable magnetic flux synchronous motors (VMFSM), which can control the magnetic flux of the PMs are intensively investigated both in industries and in academia as a next generation IPM motors [2]-[24]. The VMFSMs have been further grouped based on the location of the variable magnetic flux sources and the configurations as followings:

A) Memory motor type with variable magnetized magnets [2]-[5]

The excellent advantages in flexibly control the PM flux to achieve the most appropriate state for each operation point. However, the risk of demagnetization and the difficulty of operating point hold of a variable-magnetized magnet are concerned in the high armature magnetic flux operating point due to the opposite magnetic flux vectors against the PM magnetic flux vectors.

B) Rotor skew adjustment type with mechanical actuator [6]-[9]

These machine allows one of the rotor sections to be rotated away from the other by a servo actuator, misaligning it to reduce the flux that links the armature coils. These machines can provide good torque density and flux weakening performance, however, the added weight, power demand and complexity caused by the additional servo actuator must be considered.

C) Hybrid excitation type with PMs and field coils [10]-[15]

These machine has both sources in stator, i.e., an armature windings and a field windings, avoiding the need for slip rings. These machines show reasonable flux intensifying and weakening capabilities with variable magnetomotive force of field coils, but the additional copper loss in field coils occurs with motor efficiency drop, and an additional DC/DC converter are needed to adjust the field magnetization power of field coils.

D) Consequent pole flux path control type with field-coils [16]-[20]

These machines have no inherent risk of demagnetization with the motor configuration of constant-magnetized PMs in the rotor, and an iron pole for adjustable magnetization by field coils. On the other hand, the disadvantages are concerned in low torque density due to no available utilizing reluctance

torque. In addition, additional copper loss reduces the motor efficiency, and extra controller, i.e., DC/DC converter are required for field coils.

E) Leakage magnetic flux type [21]-[23]

These technique make into altering the leakage magnetic flux path in the flux barriers between magnet poles. The leakage magnetic flux can passively control by the magnetic flux density in [21], or actively control by inserting an iron section into the flux barrier in [22][23]. However, the narrow range of variable magnetic flux limits the extension of high efficiency area.

F) Airgap adjustment type [24]

Adjustment of the airgap length to provide field intensifying and weakening is introduced in this technique applied axial-gap machine. This technique has a good performance in terms of flux adjustment, however, the complex mechanical configuration will affect toque density and manufacturability.

To solve these problems of classic variable magnetic flux technique, a novel magnetic flux PM motor which can automatically realize the magnetic flux linkage control into armature coils without any additional actuator, any additional energy sources, and any power converter device are presented in this paper. The proposed motor requires no additional current for flux weakening control (including current vector advanced control), and no variable-magnetized magnet such as the memory motor. The operation principle of automated variable magnetic flux control is discussed, and the effect of variable magnetic flux are clarified through the adjustable speed drive characteristics. In addition, the mechanical design of the prototype are revealed, and preliminary experimental test results are demonstrated by the actual prototype machine

II. Operation Principle of Proposed Motor

A. Self-Excitation Technique of Axial-gap Wound-field rotor

The proposed synchronous motor has a toroidally-concentrated winding stator, and the torque generation surfaces are composed of three air-gaps as shown in Fig. 1. As shown in Fig. 1 (c) and (d), the armature magnetic flux occurs in a three-dimensional direction by the torus winding structure [25]. The radial-gap PM rotor and the pancake-axial-gap Wound Field (WF)-rotor rotates in synchronous speed with mechanically fastened to the output shaft. The radial-gap PM rotor has a constant-magnetized magnets on the *d*-axis, while, the axial-gap WF-rotor can be strongly magnetized with respect to rotation speed increase, because the WF-rotor has a diode rectifier circuit on the rotor and it can be automatically magnetized by the second space harmonic power which is inevitably generated by a concentrated winding structure as shown in Fig. 1 (c) and (d) [26]. Thus, an electromagnet pole of the WF-rotor is organized with respect to rotation speed increase by self-excitation technique [27]. Figure 2 (a) illustrates a simplified stator winding structure of a concentrated winding and distributed one. Fig. 2 (b) shows the magnetic flux waveforms in air-gap. As can be seen in Fig. 2, the magnetic flux waveform of the distributed winding

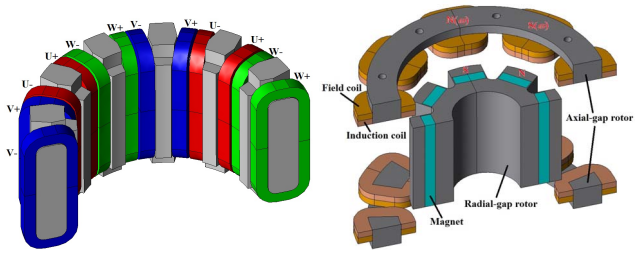

(a) Concentrated toroidal stator. (b) Axial and radial gap rotor.

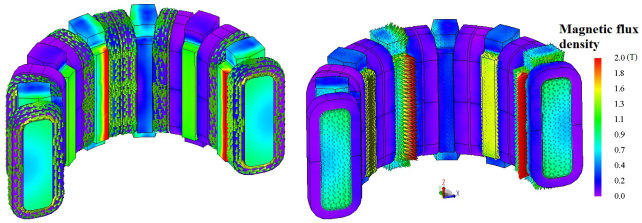

(c) Armature current vectors. (d) Magnetic flux contour and vectors.

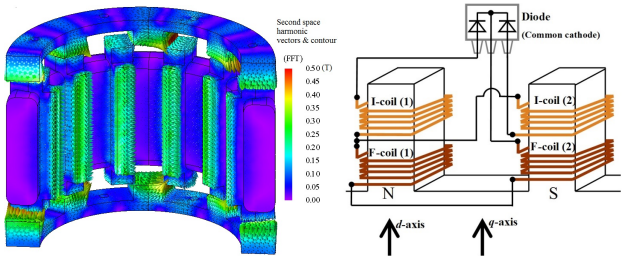

(e) Second space harmonic vectors. (d) Axial-gap WF-rotor winding circuit.

Fig. 1. Proposed motor.

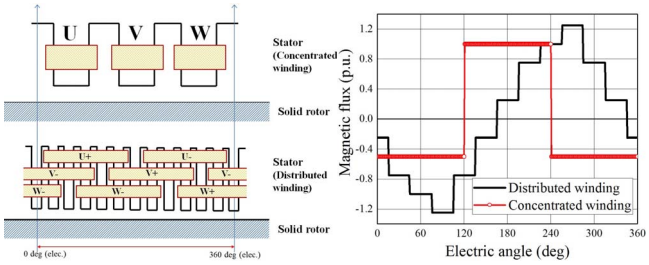

(a) Armature winding pattern. (b) Armature magnetomotive waveforms.

Fig. 2. Armature magnetomotive waveforms.

structure is basically sinusoidal, except for the slot harmonics. However, the waveform of the concentrated winding structure is distorted by the second-order harmonic component. The second-order harmonic component is caused because every phase winding is wound separately on an individual tooth without superposition on the other phase windings. Here, the relationship between a space harmonic on static coordinates and a time harmonic on the rotating reference frame are mathematically discussed. The armature currents (I_u, I_v, and I_w) and the armature magnetomotive force $F_s(t, \theta)$ can be given by

$$\begin{cases} I_u = I_a \cos(\omega t - \delta) \\ I_v = I_a \cos(\omega t - \frac{2}{3}\pi - \delta) \\ I_w = I_a \cos(\omega t - \frac{4}{3}\pi - \delta) \end{cases} \quad (1)$$

$$F_s(t,\theta) = N\left\{I_u R_s(\theta) + I_v R_s(\theta - \frac{2}{3}\pi) + I_w R_s(\theta - \frac{4}{3}\pi)\right\} \quad (2)$$

where I_a is the amplitude of armature current, ω is a angular velocity, δ is a armature current phase, N is a turn number of armature coils, θ is a spatial position, R_s is a permeance distribution coefficient. Here, as can be seen in Fig. 2 (b), the permeance distribution coefficient R_s of the concentrated winding stator, which is approximated by a fundamental and second component, can be expressed as following:

$$R_s(\theta) = R_{s1}\cos\theta + \frac{1}{2}R_{s2}\cos(2\theta - \pi) \quad (3)$$

where R_{s1}, and R_{s2} is a amplitude of the fundamental content, and a second-order space harmonic content which is superimposed on the fundamental sinusoidal waveform, respectively. Thus, Eq. (2) is derived as

$$F_s(t,\theta) = \frac{3}{2}NI_a\left\{R_{s1}\cos(\theta - \omega t + \delta) - \frac{1}{2}R_{s2}\cos(2\theta + \omega t - \delta)\right\} \quad (4)$$

As expressed in the above expression, the magnetic flux of the concentrated winding structure is composed of the two different rotating magnetic fields, i.e., the first term is the fundamental frequency, and the second term is the second-order harmonic which rotates in reverse direction against the fundamental waveform. Then, applying a rotational coordinate transform by using the relationship in synchronous rotating state as $\theta = \omega t$, the second term in Eq. (4) is observed as a third time harmonic $3\omega t$ on the dq-reference frame. Figure 3 (a) shows the rotor winding where the wound-field coils are installed to the pancake-axial-gap rotor salient poles. The rotor has two types of winding, i.e., an induction coil (I-coil) that retrieves mainly the second-space harmonic and a field coil (F-coil) for the field magnetization. The I-coil is placed around air-gap side due to the second space harmonic vector distribution as shown in Fig. 1 (e). The two coils are connected via a center-tapped full bridge diode rectifier circuit as shown in Fig. 1 (d). The field magnetization power ca be generated by the second space harmonic (third time harmonic on the dq-reference frame) linkage into the I-coil, the diode rectifier on the rotor, and the field current can be automatically obtained by self-excitation technique. The magnetomotive force of WF-rotor increases with respect to the rotation speed increase, because the self-excitation technique is based on Faraday's law. Figure 4 shows the rotor current waveforms (induced and field current) simulated by FE-analysis. By referring to rotor current waveforms in Fig. 4, the induced current flows forward and reverse at time intervals. Thus, it can be easily confirmed that the third time harmonic on the rotating reference frame (the second space harmonic on static coordinates) links to rotor windings and the electromagnet poles can be obtained by field current generated with full-bridge rectifier as shown in Fig. 1 (d).

B. Variable Magnetic Flux Technique

The unique point of the proposed motor is the magnetic pole direction between the radial-gap PM rotor and the pancake axial-gap WF-rotors. As can be seen in Fig. 5, the relationship of magnetization direction between the axial magnetic poles

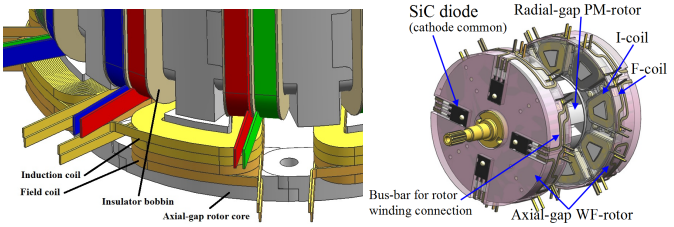

(a) Aligned rotor windings on salient pole. (b) Rotor assembly.

Fig. 3. Rotor configuration.

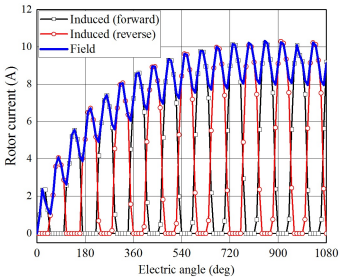

Fig. 4. Rotor current under 890 ArmsT and -20 deg for 2000 r/min.

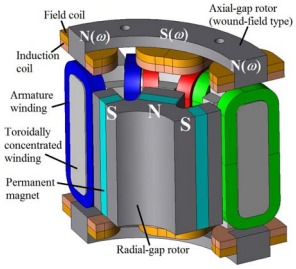

Fig. 5. Proposed motor.

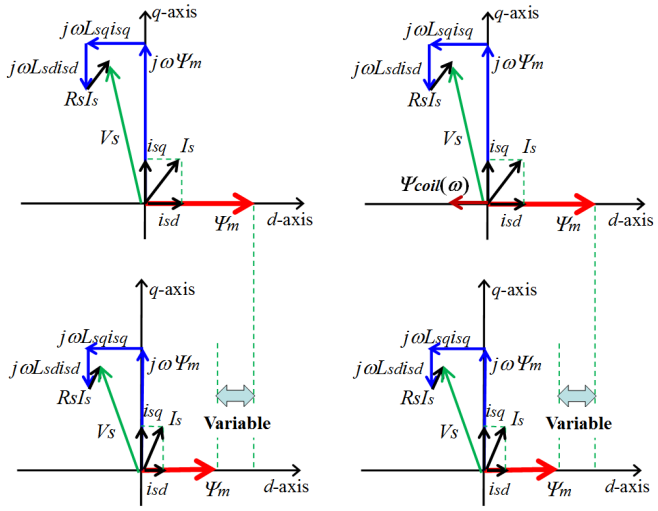

(a) Conventional. (b) Proposed.

Fig. 6. Effect of variable magnetic flux technique (Flux intensifying type).

and the radial magnetic poles is reverse (it means that an electrical skew angle is 180 deg). A schematic of the effect of variable magnetic flux technique in the case of flux intensifying type is shown in Fig. 6. As shown in Fig. 6 (a), the general variable magnetic flux technique can adjust the magnet flux ψ_m with pulse current injection or mechanical actuator; however, the proposed technique can adjust the magnet flux ψ_m by reversal electromagnet flux ψ_{coil} which is automatically magnetized in proportion to rotation speed increase.

III. Downsized Prototype Machine

A. Mechanical Design

Figure 7 (a) shows the toroidally-concentrated stator. Its core material is applied Soft Magnetic Composites (SMC) due

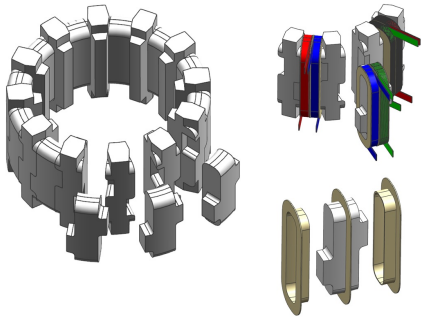

(a) Segmented stator core and torus coils with insulator bobbin.

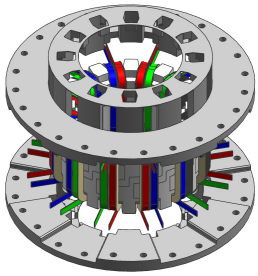

(b) Segmented stator support cover.

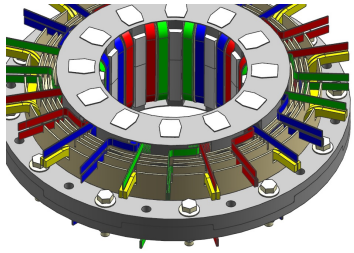

(c) Armature winding connection.

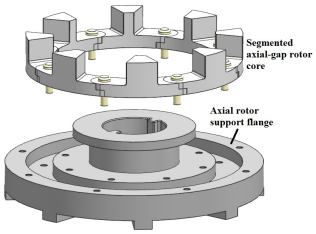

(d) Segmented axial-gap rotor and its support flange.

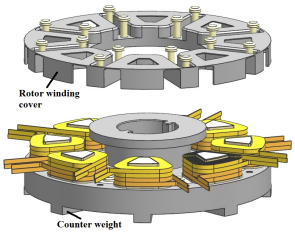

(e) Rotor winding cover.

Fig. 7. Mechanical design of prototype machine.

to three-dimensional magnetic path. Stator core is composed of 24 pieces which is segmented 12 divisions in circumferential direction, and 2 divisions in axial direction. The purpose of segmented structure is to satisfy the core piece weight density 7.4 ~ 7.5 g/cm^3 by pressing with a 100 ton press machine. An armature torus coil is preformed by edgewise winding, and installed on the stator yoke via an insulator bobbin. The segmented stator core is hold by support cover (SUS303) as shown in Fig. 7 (b), and fixed it housing by using bolt holes of stator support cover. The armature coils are connected 4 parallel per each phase by using bus bars and insulator bobbin as shown in Fig. 7 (c). Figure 7 (d) shows axial rotor configuration with segmented rotor core made by SMC material. The reason of segmented rotor core design is the same as stator core to improve its weight density in pressing process of SMC powder. The axial-gap rotor coil is preformed so as to make them flat angle alpha windings to improve the coil space factor. The I-coil is placed around the air-gap side to retrieve the space harmonics power efficiently. The both coils (I-coil and F-coil) are connected in pole-pair via a center-tapped diode module (cathode common type) as shown in Fig. 3 (b). On the other hand, the core material of radial-gap rotor is magnetic steel sheet (core thickness 0.3 mm) due to two-

Table I. Specifications of prototype.

Number of rotor poles	8
Number of stator slots	12
Motor core outer diameter	120 mm
Air-gap length	Radial 0.7 mm Axial 0.9 mm
Axial length of core	51.8 mm (without axial-gap core) 107.6 mm (with axial-gap core)
Maximum magnetomotiveforce	1272 A_{rms}T (30 s)
Number of stator coil-turn	9
Armature winding connection	4 parallel
Number of rotor induction coil-turn	30
Number of rotor field coil-turn	30
Armature coil size (with insulation coating)	5.26 mm×0.56 mm
Rotor coil size (with insulation coating)	2.57 mm×0.47 mm
Core material	SMC (stator and axial rotor) Magnetic steel sheet (radial rotor)

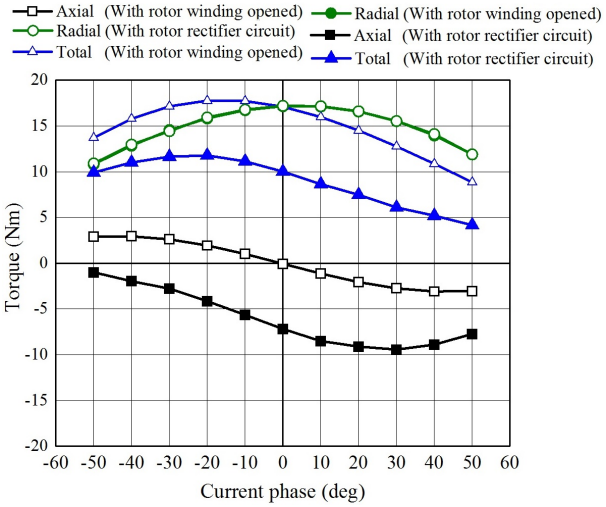

(a) Current phase-vs.-torque characteristics.

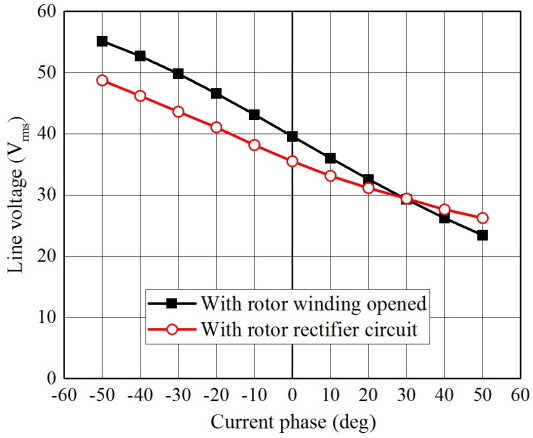

(b) Current phase-vs.-line voltage characteristics.

Fig. 8. Current phase-vs.-torque and line voltage characteristics under armature magnetomotive force 890 A_{rms}T for 3000 r/min.

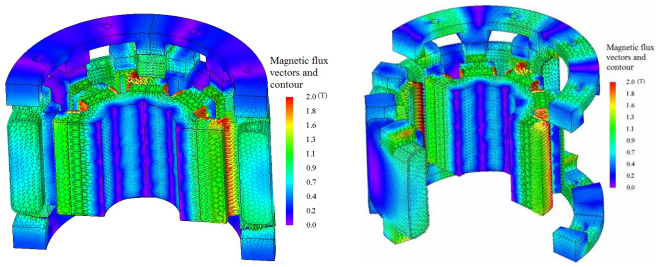

(a) Rotor winding opened. (b) Rotor winding rectified.

Fig. 9. Magnetic flux density and vectors under 890 ArmsT and current phase -20 deg for 2000 r/min.

dimensional magnetic path. Specifications of the prototype machine are listed in Table I.

B. Drive Performance Prediction by FE-analysis

Figure 8 shows current phase vs. torque and line voltage characteristics under armature magnetomotive force 890 $A_{rms}T$ for 3000 r/min. It can be easily confirmed that the axial-gap rotor torque by the E-coils greatly contributes to decrease the total output torque with self-excitation technique of reversal magnetic poles. At the same time, the armature line voltage is automatically controlled lower than rotor winding opened model by electrically reversal magnetic pole on the axial-gap rotor. In addition, the line voltage of the proposed motor can be decreased in flux intensifying area (from -90 deg to 0 deg) , however, in the flux weakening area (from 0 deg to +90deg), the line voltage is the same level compared with the conventional motor, that is without rotor circuit model (rotor winding opened). The variable magnetic flux ratio, i.e., the reduce ratio of line voltage, of proposed automatically flux weakening technique is about 16 % under MTPA point (current phase -30 deg) for 3000 r/min. Figure 9 shows the magnetic flux density and vectors compared with rotor winding opened model and rotor winding rectified model. As can be seen in this figure, it can be confirmed that the reversal magnetic pole is organized by self-excitation with utilizing second space harmonic power.

Here, the mathematical model of the proposed motor can be expressed as the following voltage equation:

$$\begin{aligned}\begin{bmatrix} v_d \\ v_q \end{bmatrix} &= \begin{bmatrix} R_s & 0 \\ 0 & R_s \end{bmatrix}\begin{bmatrix} i_d \\ i_q \end{bmatrix} + \begin{bmatrix} \mathrm{p} & -\omega \\ \omega & \mathrm{p} \end{bmatrix}\begin{bmatrix} \psi_d \\ \psi_q \end{bmatrix} \\ &= \begin{bmatrix} R_s & 0 \\ 0 & R_s \end{bmatrix}\begin{bmatrix} i_d \\ i_q \end{bmatrix} + \begin{bmatrix} L_d & 0 \\ 0 & L_q \end{bmatrix}\mathrm{p}\begin{bmatrix} i_d \\ i_q \end{bmatrix} \\ &+ \begin{bmatrix} \mathrm{p}L_d & 0 \\ 0 & \mathrm{p}L_q \end{bmatrix}\begin{bmatrix} i_d \\ i_q \end{bmatrix} + \omega\left\{\begin{bmatrix} 0 & -L_q \\ L_d & 0 \end{bmatrix}\begin{bmatrix} i_d \\ i_q \end{bmatrix} + \begin{bmatrix} 0 \\ \psi_m - \psi_{coil} \end{bmatrix}\right\}\end{aligned} \tag{5}$$

where v_d, v_q, i_d, and i_q are the d-axis, and q-axis voltages and currents, R_s is the armature winding resistance, L_d and L_q is d-axis and q-axis inductance, and p denotes a differential operator, respectively.

The output torque of the proposed motor is obtained by the vector product between the armature current and the magnetic flux, which is associated with the fourth term in Eq. (5):

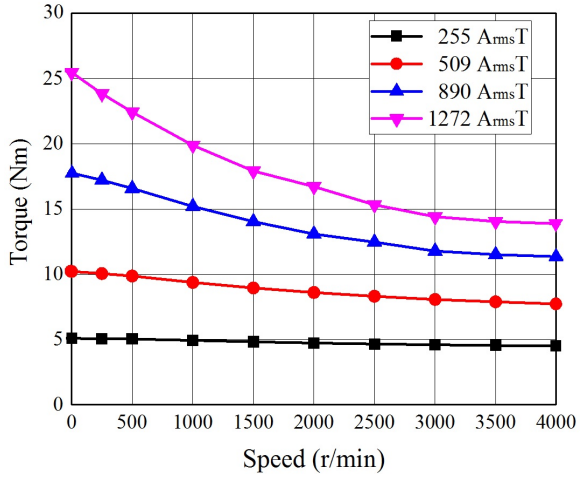

(a) Torque with respect to armature magnetomotive force increase.

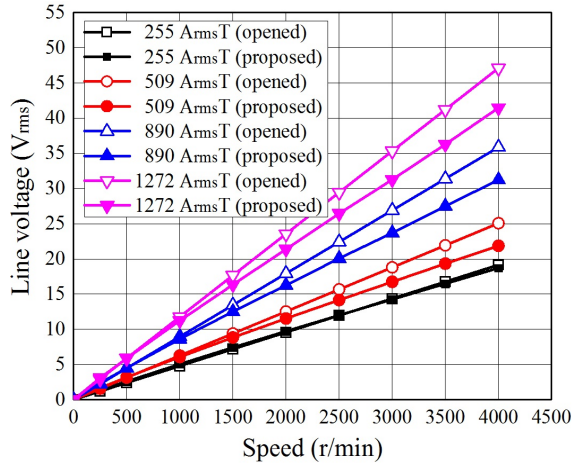

(b) Armature line voltages with respect to rotation speed increase.

Fig. 10. Adjustable speed drive characteristics under MTPA control.

$$\begin{aligned}T &= P_p\begin{bmatrix} i_d & i_q \end{bmatrix}\left\{\begin{bmatrix} 0 & -L_q \\ L_d & 0 \end{bmatrix}\begin{bmatrix} i_d \\ i_q \end{bmatrix} + \begin{bmatrix} 0 \\ \psi_m - \psi_{coil} \end{bmatrix}\right\} \\ &= P_p\left\{(L_d - L_q)i_d i_q + (\psi_m - \psi_{coil})i_q\right\}\end{aligned} \tag{6}$$

where P_p is the pole-pair number. As expressed in the above expression, the output torque is composed of the two terms, i.e., reluctance torque and the magnet torque which contains the self-excited electromagnet torque. Since the field current generating the electromagnet torque $\psi_{coil}i_q$ is proportion to ω, the proposed motor can deliver the large torque in the extremely low-speed range with radial-gap torque and pancake-axial-gap torque. On the other hand, the output torque decrease with respect to rotation speed increase due to strongly organized reversal electromagnet torque $\psi_{coil}i_q$. As expressed in Eq. (5), the line voltage also decreases simultaneously.

Figure 10 shows the adjustable speed drive characteristics under Max Torque Per Ampere (MTPA) control. When the fundamental frequency is higher, the total torque shows a characteristics to decrease because the time rate of change of the magnetic flux linked to rotor winding is increase. Thus, the induced voltage to a rotor windings increase by Faraday's law,

as a results, induced current increase, and reversal electromagnet torque increase. Furthermore, reversal electromagnet torque increase with respect to armature magnetomotive increase because the second space harmonic increase in proportion to armature magnetomotive force. In addition, it can be confirmed that the line voltages are automatically controlled to decrease without flux weakening control. From these results, the proposed motor has a potential to improve the motor efficiency by optimizing each magnetomotive force, e.g., the armature magnetomotive force, the permanent magnet flux, electromagnet flux (number of axial-rotor coil turns, and coil resistance). Furthermore, the aspect ratio between the outer diameter and the core length is also important to improve the variable magnetic flux ratio per torque. This result means that the active armature terminal voltage control, i.e., current vector control, is not needed, and be free from the iron loss increase, and an electromagnetic vibration caused by space harmonics (mainly fifth and seventh). The theoretical variable magnetic flux range is limited by approximately less than 50 %, actually less than 30 %. It is based on the fact that the second space harmonic is superimposed about a half of fundamental amplitude, a part of space harmonic is consumed by rotor coil copper loss, and the reversal electromagnet pole affect reduction of q-axis magnetic flux, i.e., torque generation content.

IV. Actual Prototype Machine

A. Prototype Machine

Figure 11 shows an actual prototype machine for principle inspection. The SMC core is formed by pressing SMC powder (Höganäs Somaloy 700 3P) under thermal steam, and finish-cutting. Preformed armature edgewise coil (AIW wire) is embedded in stator via a insulator bobbin (PPS material). The axial-gap rotor is mechanically reinforced by a resin mold (PPS) process to prevent destruction by the centrifugal force caused by a high speed rotation and to ensure electrical insulation. The diode rectifier circuit with a cathode common diode module (made by ROHM, SCS230AE2, V_R = 650 V, I_F = 15 A/leg) is mounted on the rotor via a diode holder (PPS). The magnetic steel sheet of radial-gap rotor core is selected 30DH made by nippon steel, and the permanent magnet material is Nd-Fe-B magnet (B_r = 1.22 T, H_{cb} = 965.7 kA/m @ 293 K). As shown in Fig. 11 (h), the search coils (ϕ0.16, 8 turn) are wound on the armature coils to monitor the line voltage decrease ratio, experimentally.

B. Preliminary Experimental Tests

In a preliminary experimental test, the principle of self-excitation technique utilizing space harmonics which is automatically generated by concentrated winding structure is demonstrated. The rotor induced current in the diode forward direction and the reverse direction for one pole pair is measured with a slip-ring to demonstrate the self-excitation by the third time harmonic as shown in Fig. 12. Figure 13 shows the stator armature current (U-phase) and rotor current waveforms (induced current in forward and reverse direction) for 1800 r/min under 405 $A_{rms}T$ of the armature magnetomotive force. The inverter carrier frequency is set at

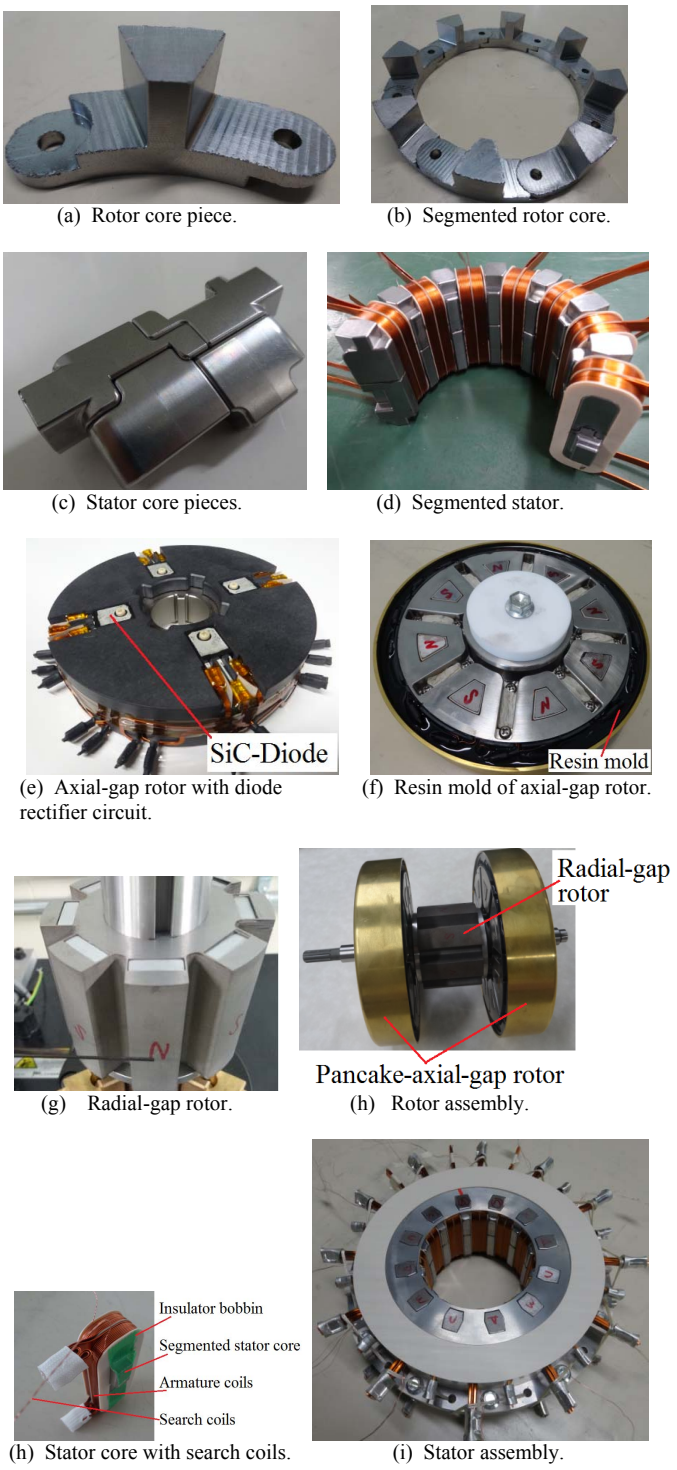

(a) Rotor core piece. (b) Segmented rotor core.
(c) Stator core pieces. (d) Segmented stator.
(e) Axial-gap rotor with diode rectifier circuit. (f) Resin mold of axial-gap rotor.
(g) Radial-gap rotor. (h) Rotor assembly.
(h) Stator core with search coils. (i) Stator assembly.

Fig. 11. Actual prototype machine.

12 kHz, and used universal inverter (Myway plus, pMotion). In the experimental test, the load test of the motor is limited in the low-speed range (under 2000 r/min) and low-armature magnetomotive force (under 405 $A_{rms}T$) due to the capable maximum speed and mechanical stress of slip-ring. By referring to rotor current waveforms in Fig. 13, the induced current flows forward and reverse at time intervals. Thus, it can be easily confirmed that the third time harmonic on the

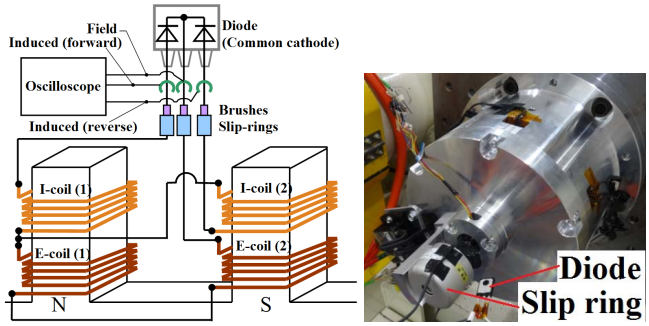

(a) Rotor current measurement method. (b) Prototype with slip-ring.

Fig. 12. Rotor current measurement method.

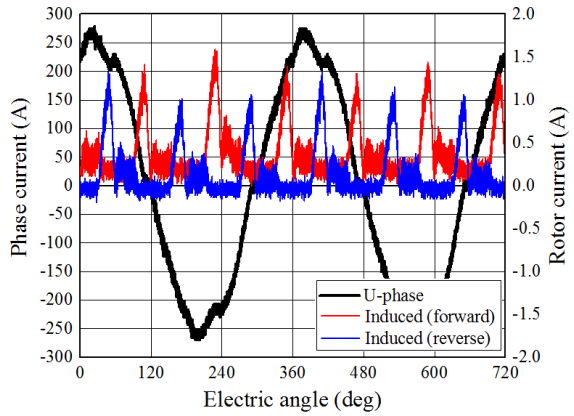

Fig. 13. Armature current and rotor induced currents under 405 $A_{rms}T$, and current phase -20 deg for 1800 r/min.

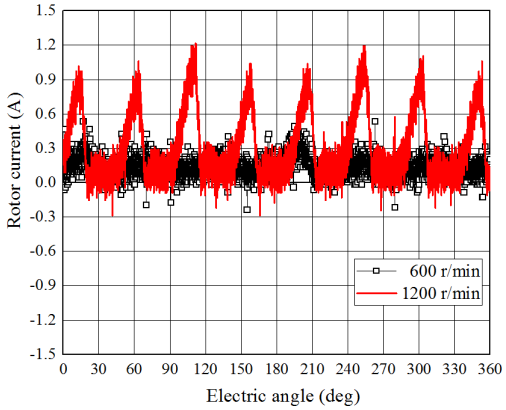

Fig. 14. Rotor field current under 405 ArmsT and current phase -20 deg for 600 r/min and 1200 r/min.

rotating reference frame (the second space harmonic on static coordinates) links to rotor windings and the electromagnet poles can be obtained by field current generated with full-bridge rectifier as shown in Fig. 12. Figure 14 shows the rotor field currents under 405 $A_{rms}T$ and current phase -20 deg for 600 r/min, and 1200 r/min. As can be seen in this figure, it can be easily confirmed that the field current increases in proportion to rotation speed increase. On the other hand, a large rotor field current ripple is observed in experimental condition. This reason is that the induced voltages by space harmonics is low under the armature magnetomotive force 405$A_{rms}T$, and almost of its voltages are wasted in rotor cupper loss. However, the stable field current will be obtained in more higher rotation speed condition and magnetomotive force.

V. Conclusion

This paper has presented a newly variable magnetic flux PM motor with self-excited wound-field magnetomotive force by the space harmonics. The advantage of the automatically electrified reversal magnetic pole concept has been clarified through the FE-analysis. In addition, verification of the self-excitation principle generated by the space harmonics power has been investigated through the mathematical model and FE-analysis. Furthermore, the downsized actual prototype machine design is revealed, and the self-excited rotor current is experimentally demonstrated via a slip-ring. The future work of this study is to demonstrate the experimental test, e.g., current phase vs. torque characteristics, adjustable speed drive characteristics, and efficiency maps. And it is important to clarify the advantages of the variable magnetic concept with automatically electrified reversal magnetic pole compared with conventional constant magnetized PM synchronous motor (rotor winding opened model).

References

[1] United States Environmental Protection Agency (EPA) accessed on 24. AUG. 2015
http://www2.epa.gov/science-and-technology/sustainable-practices-science

[2] Ostovic, V.: "Memory Motors", *IEEE Industry Applications Magazine,* vol. 9, pp.52-61 (2003)

[3] Ostvic, V.: "Memory Motors - a New Class of Controllable Flux PM Machines for a True Wide Speed Operation", *Proc. of IEEE Industry Aplications Society Conference 2001*, vol. 4, p. 2577-2584 (2001)

[4] K. Sakai, K. Yuki, Y. Hashiba, N. Takahashi, K. Yasui, and L. Kovudhikulrungsri: "Principle and Basic Characteristics of Variable Magnetic-Force Memory Motors", *IEEJ Trans. on IA*., vol. 131, No. 1, pp.53-60 (2011) (in Japanese)

[5] T. Kato, N. Linsuwan, C. Y. Yu, K. Akatsu, and R. D. Lorenz: "Rare Earth Reduction Using a Novel Variable Magnetomotive Force, Flux Intensified IPM Machine", *IEEE Trans. on IA*., vol. 50, No. 3, pp. 1748-1756 (May/June, 2016)

[6] T. Nonaka, S. Oga, and M. Ohto: "Consideration about the Drive of Variable Magnetic Flux Motor", *IEEJ Trans. on IA*., vol. 135, No. 5, pp. 451-456 (2015) (in Japanese)

[7] F. Caricchi, F. Crescimbini, F. G. Capponi, and L. Solero: "Permanent-Magnet, Direct-drive, Starter/Alternator Machine with Weakened Flux Linkage for Constant-power Operation over Extremely Wide Speed Range", *Conference Record of the 2001 IEEE IA. Conference 2001. Thirty-Sixth IAS Annual Meeting*, vol. 3, pp. 1626-1633 (Sept/Oct, 2016)

[8] L. D. Ferraro, F. Caricchi, and F. G. Capponi: "Analysis and Comparison of a Speed-dependant and a Torque-dependant Mechanical Device for Wide Constant Power Speed Range in AFPM Stator/Alternators", *IEEJ Trans. on PE*., vol. 21, No. 3, pp. 720-729 (May, 2006)

[9] G. Zhou, T. Miyazaki, S. Kawamata, D. Kaneko, and N. Hino: "Development of Variable Magnetic Flux Motor Suitable for Electric Vehicle", *IEEE 2010 International Power Electronics Conference (IPEC)*, pp. 2171-2174 (June, 2010)

[10] T. Kosaka, Y. Kano, N. Matsui, and C. Pollock: "A Novel Multi-Pole Permanent Magnet Synchronous Machine with SMC Bypass Core for Magnet Flux and SMC Field-pole core with Toroidal Coil for Independent Field Strengthening/Weakening", *IEEE 2005 European Conference on Power Electronics and Applications*, pp. 10-, (Sept, 2005)

[11] I. Ozawa, T. Kosaka, and N. Matsui: "Less Rare-earth Magnet-high Power Density Hybrid Excitation Motor Designed for Hybrid Electric Vehicle Drives", *IEEE 2009 European Conference on Power Electronics and Applications (EPE'09),* pp. 1-10 (Sept, 2009)

[12] F. Leonardi, T. Matsuo, Y. Li, T. A. Lipo, and P. McCleer: "Design Considerations and Test Results for a Doubly Salient PM Motor with Flux Control", *Industry Applications Conference, 1996. Thirty-First IAS Annual Meeting, IAS '96., Conference Record of the 1996 IEEE,* vol. 1, pp. 458-463 (Oct, 1996)

[13] Y. Li, and T. A. Lipo: "A Doubly Salient Permanent Magnet Motor Capable of Field Weakening", *Power Electronics Specialists Conference, 1995. PESC '95 Record., 26th Annual IEEE*, vol. 1, pp. 565-571 (Jun, 1995)

[14] D. Fodorean, A. Djerdir, I. A. Viorel, and A. Miraoui: "A Double Excited Synchronous Machine for Direct Drive Application – Design and Prototype Tests", *IEEE Trans. on Energy Conversion*, vol. 22, No. 3, pp. 656-665 (Sept, 2007)

[15] J. Oyama, T. Abe, T. Higuchi, and E. Yamada: "Steady-state Characteristics of a Half-wave Rectified Brushless Synchronous Motor with Permanent Magnet", *IEEJ Trans. on IA.*, vol. 109, No. 7, pp. 507-514 (1989) (in Japanese)

[16] T. Mizuno, K. Nagayama, T. Ashikawa, and T. Kobayashi: "Basic Principles and Characteristics of Hybrid Excitation Type Synchronous Machine", *IEEJ Trans. on IA*., vol. 115, No. 11, pp. 1402-1411 (1995) (in Japanese)

[17] M. Aydin, S. Huang, and T. A. Lipo: "A New Axial Flux Surface Mounted Permanent Magnet Machine Capable of Field Control", *Conference Record of the Industry Aplications Conference, 2002. 37th IAS Annual Meeting*, vol. 2, pp. 1250-1257 (2002)

[18] J. A. Tapia, F. Leonardi, and T. A. Lipo: "Consequent-Pole Permanent-Magnet Machine with Extended Field-Weakening Capability", *IEEE Trans. on IA*., vol. 39, No. 6, pp. 1704-1709 (2003)

[19] M. Namba, K. Hiramoto, and H. Nakai: "Novel Variable-Field Motor with a Three-Dimentional Magnetic Circuit", *IEEJ Trans. on IA*., vol. 135, No. 11, pp. 1085-1090 (2015) (in Japanese)

[20] T. Ogawa, T. Takahashi, M. Takemoto, H. Arita, A. Daikoku, and S. Ogasawara: "The Consequent-Pole Type Ferrite Magnet Axial Gap Motor with Field Winding for Traction Motor Used in EV", *SAEJ Proc. of EVTeC & APE Japan 2016*, No. 20169094 (2016)

[21] T. Kato, M. Minowa, H. Hijikata, and K. Akatsu: "High Efficiency IPMSM Effectively Utilizing Variable Leakage Flux Characteristics", *IEEJ JIASC 2014*, No. 3-13, pp. 139-142 (2014) (in Japanese)

[22] I. Urquhart, D. Tanaka, R. Owen, Z. Q. Zhu, J. B. Wang, and D. A. Stone: "Mechanically Actuated Variable Flux IPMSM for EV and HEV Applications", Proc. of EVS27 *International Battery, Hybrid and Fuel Cell Vehicle Symposium 2013*, pp. 684-695 (2013)

[23] K. Baoquan, L. Chunyan, and C. Shukang: "A New Flux Weakening Method of Permanent Magnet Synchronous Machine", *Proc. of Eighth International Conference on Electrical Machines and Systems, 2005. ICEMS 2005*, vol. 1, pp. 500-503 (Sept, 2005)

[24] H. Nakai, K. Hiramoto, Y. Otani, and Y. Inaguma: "Novel Field Weakening Control Method for an Axial Flux Permanent Magnet Motor Using an Adjustable Gap Length", *IEEJ JIASC*, No. 364, pp. 337-342 (2007) (in Japanese)

[25] M. Aoyama, K. Nakajima, and T. Noguchi : "Proposal of Electrified Reversal Magnetic Pole Type Variable Magnetic Flux Motor", *IEEJ Annual Meeting 2016*, No. 5-043, pp. 77-78 (2016) (in Japanese)

[26] M. Aoyama, and T. Noguchi : "Experimental Verification of Radial-Air-Gap-Type Permanent-Magnet-Free Synchronous Motor Utilizing Space Harmonics with Auxiliary Poles", *IEEJ Trans. on IA.*, vol. 135, No. 8, pp. 869-881 (2015) (in Japanese)

[27] S. Nonaka : "The Self-Excited Type Single-Phase Synchronous Motor ", *IEEJ Trans. IA*, Vol. 78, No. 842, pp. 1430-1438 (1958-11) (in Japanese)